Title

Grasses use an alternatively wired bHLH transcription factor network to establish stomatal identity

Journal

Proceedings of the National Academy of Sciences of the United States of America, 113(29)

ISSN

0027-8424

Authors

Raissig, Michael T
Abrash, Emily
Bettadapur, Akhila
et al.

Publication Date

2016-07-19

DOI

10.1073/pnas.1606728113

Peer reviewed

Grasses use an alternatively wired bHLH transcription factor network to establish stomatal identity

Michael T. Raissig[a,1], Emily Abrash[a,1], Akhila Bettadapur[b], John P. Vogel[c], and Dominique C. Bergmann[a,b,2]

[a]Department of Biology, Stanford University, Stanford, CA 94305; [b]Howard Hughes Medical Institute, Stanford University, Stanford, CA 94305; and [c]Department of Energy Joint Genome Institute, Walnut Creek, CA 94598

Edited by Richard Scott Poethig, University of Pennsylvania, Philadelphia, PA, and approved June 2, 2016 (received for review April 27, 2016)

Stomata, epidermal valves facilitating plant–atmosphere gas exchange, represent a powerful model for understanding cell fate and pattern in plants. Core basic helix–loop–helix (bHLH) transcription factors regulating stomatal development were identified in *Arabidopsis*, but this dicot's developmental pattern and stomatal morphology represent only one of many possibilities in nature. Here, using unbiased forward genetic screens, followed by analysis of reporters and engineered mutants, we show that stomatal initiation in the grass *Brachypodium distachyon* uses orthologs of stomatal regulators known from *Arabidopsis* but that the function and behavior of individual genes, the relationships among genes, and the regulation of their protein products have diverged. Our results highlight ways in which a kernel of conserved genes may be alternatively wired to produce diversity in patterning and morphology and suggest that the stomatal transcription factor module is a prime target for breeding or genome modification to improve plant productivity.

stomatal development | bHLH transcription factor | *Brachypodium* | grass

Stomata are valves on the surface of plants with central roles in gas exchange and biosphere productivity. Stomata are both ancient—they appear on 400 million-year-old fossils—and nearly ubiquitously found in extant land plants. The diversity of stomatal morphologies and patterned distributions across different plant families coupled with rapidly advancing functional genomic resources offers a powerful opportunity to follow morphological innovation and gene regulatory network evolution simultaneously. In most plants, stomata consist of two kidney-shaped epidermal guard cells (GCs) surrounding a pore (Fig. 1*A*). Grass stomatal morphology is unique, featuring dumbbell-shaped GCs flanked by subsidiary cells (SCs) (Fig. 1*A*), and physiological measurements suggest this derived form is more efficient (1). The distribution of stomata on leaves is also species specific. Dicots such as *Arabidopsis* display a scattered distribution, with avoidance of direct contact being the most basic patterning rule; dispersed stem cell-like stomatal precursors divide throughout the leaf to produce this pattern and promote the typical "broadleaf" or radial growth characteristic of these plants (Fig. 1*A*). Grasses, in contrast, generate stomata, which are always oriented in the same direction, from specific cell files. These stomatal lineage files are established in a single zone at the leaf base with differentiation proceeding in a linear gradient toward the tip (Fig. 1*A*).

Our understanding of the genetic underpinnings of stomatal fate and pattern is derived mostly from studies in the dicot *Arabidopsis* where the group Ia basic helix–loop–helix (bHLH) transcription factors *SPEECHLESS* (*AtSPCH*), *AtMUTE*, and *AtFAMA* establish stomatal lineage identity, regulate the transition to terminal precursor fate, and promote the differentiation of GCs, respectively (2–4). The function of these stage-specific factors requires heterodimerization with one of two largely redundant bHLH group III partners, *INDUCER OF CBF EXPRESSION1* (*ATICE1*) and *AtSCREAM2* (*SCRM2*) (5). Local cell–cell communication to establish the pattern is mediated by peptide–receptor signaling transduced through a MAPK cascade (reviewed in ref. 6), and AtSPCH is a direct target of this posttranslational regulation (7). Homologs of the group Ia and group III bHLHs are widespread among stomata-producing plants but have not been identified in the genomes of lineages lacking stomata such as algae and the liverwort *Marchantia* (8). Secondary loss of stomata, as in the seagrass *Zostera marina*, is accompanied by loss of *SPCH*, *MUTE*, *FAMA*, and *SCRM2* orthologs (9).

The grasses are key species for food, fuel, and the global environment. The remarkable success of these plants has been attributed to improved photosynthesis through the developmental innovations of bundle sheath cells (10) and highly responsive stomata consisting of GCs in intimate connection with flanking SCs (1). The recruitment of SCs requires intercellular signaling and cortical actin regulation in maize (11–13), and in rice, final GC differentiation requires *OsFAMA* (14), but how the stomatal lineage is initiated and patterned and what factors regulate the behavior of precursor cell types in grasses is completely unknown.

Here we show that stomatal initiation in the wheat relative *Brachypodium distachyon* uses orthologs of bHLH transcription factors known from *Arabidopsis*, but the function and behavior of individual genes, the regulation of their protein products, and the overall form of their interacting regulatory networks have diverged between the plant groups. Our results demonstrate how a conserved stomatal module is alternatively wired to accommodate the different modes of stomatal initiation associated with different leaf-patterning programs.

Results

Isolation of a *Brachypodium* Mutant Lacking Stomata and Identification of the Causal Gene as *BdICE1*. As is typical among grasses, stomatal precursors are first evident at the base of the *Brachypodium* leaf as more frequently dividing cell files (Fig. 1*B*). Cells in these files

Significance

Plants both control and are controlled by the global climate. Grasses in natural and agricultural systems participate in the exchange of atmospheric CO_2 for biosphere-derived oxygen and water vapor via microscopic epidermal valves (stomata), but how these stomata are made in grasses is unknown. Using genetic screens and targeted genome editing, we identify and characterize master transcriptional regulators of stomatal initiation in the wheat relative *Brachypodium*. Surprisingly, the unique stomatal form and pattern of grasses is regulated by orthologs of *Arabidopsis* stomatal basic helix–loop–helix (bHLH) transcription factors, although the function of individual genes and regulation of their protein products have diverged. This finding suggests that the stomatal core bHLH transcription factors are excellent breeding targets to enhance performance in grasses.

Author contributions: M.T.R., E.A., and D.C.B. designed research; M.T.R., E.A., and A.B. performed research; J.P.V. contributed new reagents/analytic tools; M.T.R., E.A., and D.C.B. analyzed data; and M.T.R., E.A., and D.C.B. wrote the paper.

The authors declare no conflict of interest.

This article is a PNAS Direct Submission.

Freely available online through the PNAS open access option.

[1]M.T.R. and E.A. contributed equally to this work.

[2]To whom correspondence should be addressed. Email: dbergmann@stanford.edu.

This article contains supporting information online at www.pnas.org/lookup/suppl/doi:10.1073/pnas.1606728113/-/DCSupplemental.

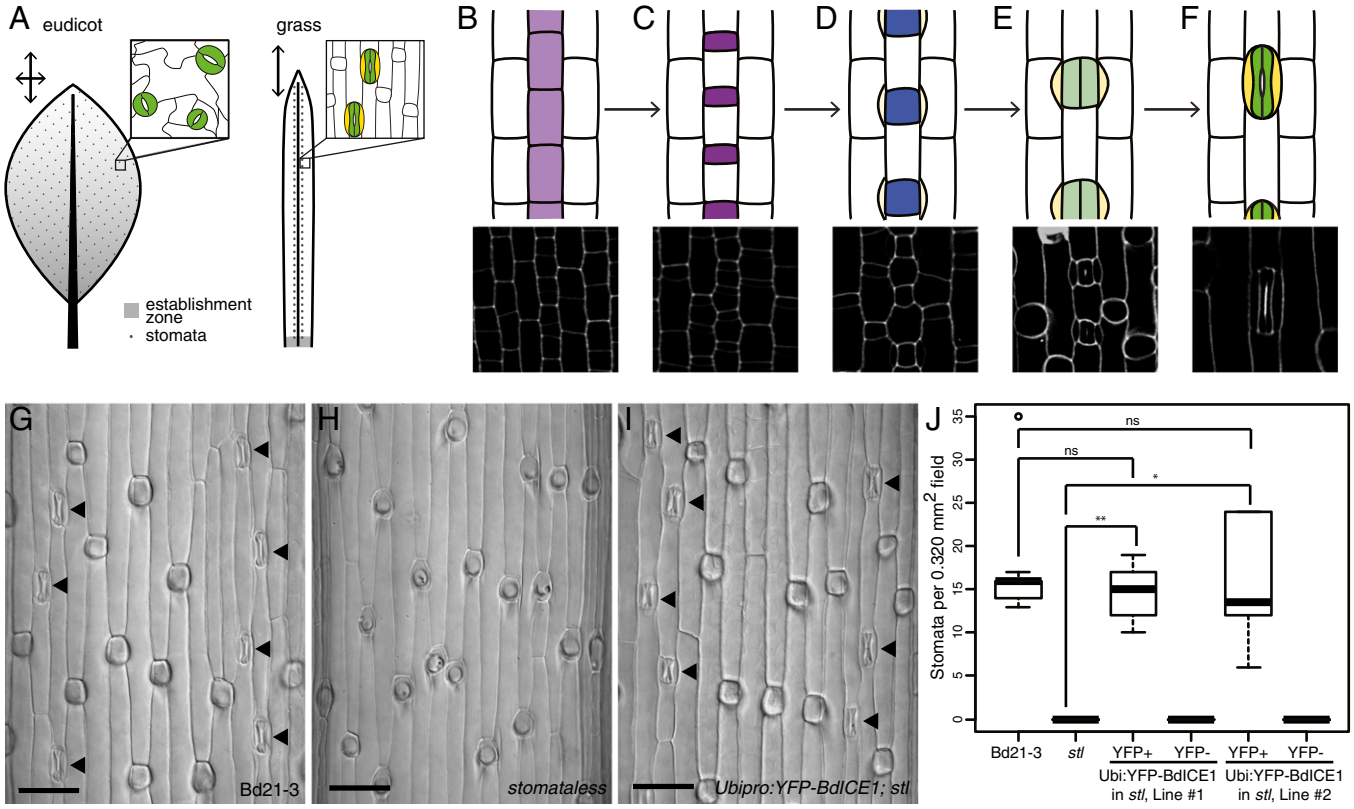

Fig. 1. Stomatal development in *Brachypodium* requires *BdICE1*. (*A*) Stomatal production in eudicot leaves where stomatal stem cell populations are dispersed throughout the epidermis and stomata are randomly oriented (*Left*) and in grass leaves that exhibit a longitudinal gradient of development with divisions restricted to the leaf base and differentiation toward tip (*Right*). Grass stomata are restricted to specific files and all have the same orientation. Boxes highlight typical eudicot stomata consisting of two GCs (green) surrounding a pore (*Left Box*) and the typical four-celled grass stomata of two GCs (green) flanked by two SCs (yellow) (*Right Box*). (*B–F*) Diagrams and confocal images of *Brachypodium* stomatal development; these and all subsequent images represent the five main developmental stages, with the youngest at the left and cells toward the base of the leaf at the bottom. Stomatal cell files are established early and proliferate to make smaller cells (light purple) (*B*) and divide asymmetrically to produce GMCs (dark purple) (*C*). GMCs mature (blue) and recruit SCs (yellow) (*D*). GMCs divide symmetrically once (*E*) and differentiate to GCs (green) (*F*). Cell walls are stained with PI in confocal images. (*G*) DIC image of cleared WT (Bd21-3) epidermis. (*H*) *stl* epidermis. (*I*) Epidermis of *stl* complemented with *Ubipro:YFP-BdICE1*. Black arrowheads indicate stomata. All DIC images display abaxial first leaves, 6 dpg. (*J*) Quantification of stomatal density per field of view in WT (Bd21-3), *stl*, and *stl*; *Ubipro:YFP-BdICE1* (lines #1 and #2). We analyzed the abaxial first leaf of 6-dpg T1 plants (progeny of initial transformed regenerants). Six individuals were analyzed per group, except for YFP$^-$ line #2, which had only one T1 and was excluded from statistical analysis. In the boxplots, the black horizontal line indicates the median; upper and lower edges of the box are the upper and lower quartiles; whiskers extend to the largest observation within 1.5 interquartile ranges of the box; circles indicate outliers. (Scale bars: 50 μm.) *$P < 0.05$, **$P < 0.01$.

undergo one asymmetric division (Fig. 1*C*), with the smaller daughter cells becoming stomatal precursors (guard mother cells or GMCs) (Fig. 1*D*) that recruit SCs by inducing oriented asymmetric divisions in their lateral neighbors (Fig. 1*D*) (11–13). Following SC recruitment, GMCs divide symmetrically (Fig. 1*E*), and their daughters differentiate into dumbbell-shaped GCs (Fig. 1*F*). Each of these stages is likely to be subject to multiple regulatory inputs. We were particularly interested in stomatal lineage identity and initiation, and because loss of stomata is typically lethal (2–4), we created and screened an ethyl methanesulfonate (EMS)-mutagenized population for phenotypes on the first leaves of seedlings grown on nutrient agar and used a pooling strategy to enable recovery of lethal mutants from heterozygous siblings. We identified *stomataless* (*stl*), a recessive mutant completely lacking stomata (Fig. 1 *G* and *H*). Although *stl* leaves have no GCs or SCs, they do possess normal nonstomatal epidermal cells such as hairs, pavement cells, and vein-associated silica cells (Fig. 1 *G* and *H*), indicating that the mutant affects a gene specifically required to produce stomata. Plate-grown *stl* mutants arrest as pale green seedlings, presumably because of carbon starvation. Based on previous work in *Arabidopsis*, the obvious candidates to yield this phenotype were *BdSPCH1* or *BdSPCH2*, the duplicated *AtSPCH* homologs (3); however, we found no mutations associated with these loci in *stl* plants. A stomataless phenotype in *Arabidopsis* also can result from the loss of both *AtICE1* and *AtSCRM2* (5); therefore we sequenced both *BdICE1* and *BdSCRM2*. The *BdSCRM2* locus was wild-type (WT), but *stl* plants contain an early nonsense mutation in *BdICE1* (Fig. S1*A*). We confirmed that the *BdICE1* mutation was causal by complementation of the *stl* stomatal and lethality phenotypes by *Ubipro:YFP-BdICE1* (two independent T1 lines) (Fig. 1 *I* and *J*). Hereafter, we refer to the original mutant line as "*stl*" and the gene product as "BdICE1."

In *Arabidopsis*, *AtICE1* and *AtSCRM2* act redundantly (5) and are also part of a Brassicaceae-specific duplication (Fig. S2). The simple explanation for why loss of *BdICE1* alone yields the *stl* phenotype is that the earlier grass-specific duplication of *BdICE1* and *BdSCRM2* produced true paralogs and that *BdSCRM2* acquired a different, nonstomatal function. When we generated a *BdSCRM2pro:YFP-BdSCRM2* reporter, however, it was clearly and specifically expressed within the stomatal lineage (Fig. 2 *A–E*). Moreover, this construct was sufficient to generate some stomata in *stl*/*bdice1* (Fig. S3), and overexpression (*Ubipro:YFP-BdSCRM2*) significantly rescued the *stl*/*bdice1* phenotype (Fig. S3).

To characterize the endogenous role of *BdSCRM2*, we generated *bdscrm2* mutant plants using clustered, regularly interspaced short palindromic repeats (CRISPR)–CRISPR-associated 9 (Cas9) genome editing (Fig. 2*F*) (15). Like *stl*/*bdice1* plants, plants bearing

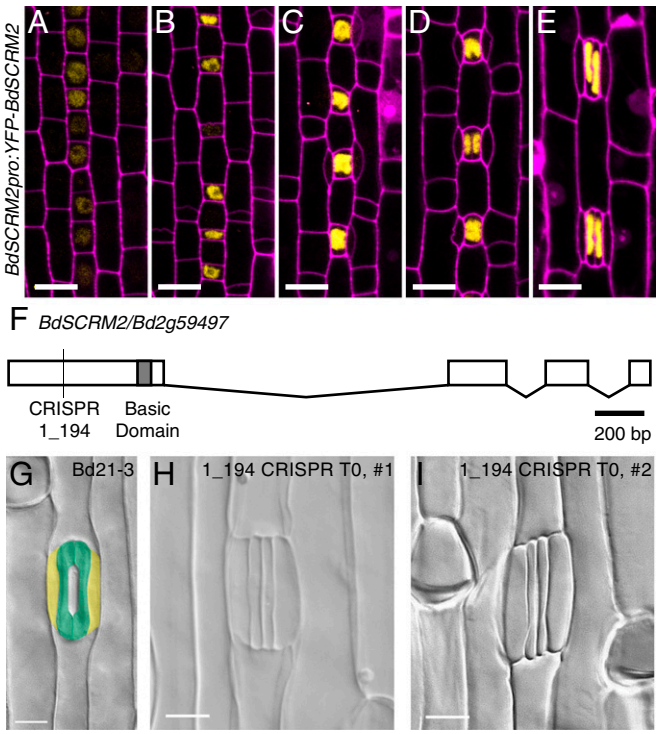

Fig. 2. *BdSCRM2* is expressed throughout the stomatal lineage but is required only for differentiation of mature stomata. (*A–E*) Expression of *BdSCRM2pro:YFP-BdSCRM2:BdSCRM2term* in the early, specified stomatal cell file (*A*), in young GMCs (*B*), in mature GMCs during SC recruitment (*C*), in dividing GMCs (*D*), and in mature stomata (*E*). All confocal images show the third leaf of a T1 plant at 11 dpg. Cell walls were stained with PI. (*F*) Gene model of *BdSCRM2* showing the site of CRISPR targeting (vertical line) and the basic domain (gray). (*G*) WT (Bd21-3) stomata showing two dumbbell-shaped GCs (false-colored green) flanked by two SCs (false-colored yellow). (*H* and *I*) Arrested four-cell complex in two independent *bdscrm2* lines. DIC images show the abaxial first leaf of T0 plants at 6–8 dpg. (Scale bars: 10 μm.)

nonsense mutations (Fig. S4*A*) in *BdSCRM2* were seedling lethal. Interestingly, *BdSCRM2* mutant leaves did produce four-celled complexes in the normal locations of stomata, but the GCs failed to mature correctly (Fig. 2 *G–I*), indicating that *BdSCRM2* is required for a late stage in stomatal differentiation and function. Thus, despite originating from distinct duplication events in grasses and Brassicaceae, both paralogs in each species were recruited for stomatal development, although their individual contributions to stomatal development differ.

***BdSPCH1* and *BdSPCH2* Are Redundantly Required for Stomatal Lineage Identity.** The novel and nonredundant roles of *BdICE1* and *BdSCRM2* in stomatal initiation and GC maturation, respectively, prompted us to consider the roles of the duplicated *AtSPCH* orthologs *BdSPCH1* and *BdSPCH2*. The duplication itself is interesting, because grasses do not have the self-renewing (meristemoid) phase for which *AtSPCH* is the single dedicated regulator (3).

The translational reporter *BdSPCH1pro:BdSPCH1-YFP* is seen exclusively within the stomatal lineage, and expression peaks in mature GMCs, but it shows very weak, patchy expression at early stages (Fig. 3*A*). *BdSPCH2pro:BdSPCH2-YFP*, in contrast, strongly and consistently marks stomatal cell files from the earliest observable stage through mature GMCs (Fig. 3*B*). We gene-edited both loci using CRISPR-Cas9 (Fig. 3 *C* and *D*) (15). Although *bdspch1* mutants showed only a small reduction in stomatal density (Fig. S5 *B–D*), *bdspch2* plants produced dramatically fewer stomata (Fig. S5 *E–K*). When we crossed the predicted null alleles *bdspch1-2* and *bdspch2-1*, we identified three phenotypic classes among F2 plants: approximately WT stomatal density, low stomatal density, and stomataless (Fig. 3 *E–H*). The stomataless phenotypic class represented ∼1/16th of the F2 progeny ($n = 5$ of 89) (Fig. 3 *E–H*), and genotyping of three stomataless individuals confirmed homozygous 2-bp deletions in both *BdSPCH1* and *BdSPCH2* (Fig. S4*B*). Together, these results suggest that *BdSPCH2* and *BdSPCH1* have overlapping functions in establishing stomatal fate, but *BdSPCH2* has a more prominent role, consistent with the timing and the expression levels of the translational reporters and the phenotype of the single mutants (Fig. 3 *A* and *B* and Fig. S5).

Loss of stomata could arise from failures in stomatal cell file specification or later in stomatal cell fate acquisition or maintenance, so we tested when the *stl* and *bdspch1 bdspch2* defects arise. Nascent stomatal cell files are distinguished by their distinctly smaller cells and are found at a stereotyped distance from veins at the base of young leaves [second leaf, 7 d postgermination (dpg)] (Fig. S6*A*). The *stl* or *bdspch1 bdspch2* mutant leaves, however, do not produce files of small cells in these positions, suggesting that stomatal files are never established (Fig. S6 *B* and *C*). In both *Arabidopsis* and *Brachypodium*, therefore, *SPCHs* and *ICE1* function in the initiation of the stomatal lineage.

Posttranslational Regulation and Relationships Among Stomatal bHLHs Diverge Between Species. In *Arabidopsis* stomatal lineage initiation, regulatory interactions place *AtSPCH* upstream and responsible for the expression of *AtICE1*/*AtSCRM2*, whose products, as dimerization partners of AtSPCH, promote SPCH stability (16). Are these relationships conserved in the *Brachypodium* gene network? We first assayed gene expression in various WT tissues to get a reporter-independent measure of relative transcript abundances. *BdICE1*, *BdSPCH1*, and *BdSPCH2* are each expressed primarily in the leaf division zone, with dramatically less transcript in mature leaves and roots (Fig. S7*A*). Although *AtSPCH* exhibits this pattern, *AtICE1* is broadly expressed and has roles outside of stomatal development (17). We then tested whether expression dependency relationships were conserved by measuring *BdICE1*, *BdSPCH1*, and *BdSPCH2* transcripts in the division zone of *bdspch1 bdspch2* and *stl* leaves. In contrast to the situation in *Arabidopsis*, where stomatal lineage *ICE1* and *SCRM2* expression depends on SPCH, we could detect *BdICE1* transcripts in *bdspch1 bdspch2* mutants and *BdSPCH1* and *BdSPCH2* transcripts in *stl* mutants (Fig. S7*B*), indicating at least partial transcriptional independence. We did observe considerable variation in transcript levels of all three genes when measured in mutant backgrounds (Fig. S7), suggesting that there may be a mutual requirement for stabilization of gene expression.

In *Arabidopsis*, ICE1/SCRM2 can be overexpressed to generate excessive stomata, but overexpression of *SPCH* has little effect because posttranslational modifications lead to its degradation (3, 7). Interestingly, this regulatory strategy appears reversed in *Brachypodium*. Broad and high-level expression (Ubi promoter) resulted in the appearance of *BdSPCH1-YFP* and *BdSPCH2-YFP* throughout the leaf (Fig. 3*I* and Fig. S8) and the induction of many additional cell divisions in the epidermis (Fig. 3*J* and Fig. S8). Strong *Ubipro:BdSPCH2-YFP* lines produced ectopic stomatal complexes, likely by reprogramming hair cell precursors and inducing division and pore formation within young hairs (Fig. 3 *J* and *K* and Movies S1 and S2). In contrast, when expressed with the same Ubi promoter, the accumulation of *Ubipro:ICE1-YFP* (Fig. S1 *B–F*) and *Ubipro:SCRM2-YFP* (Fig. S1 *G–K*) was restricted to the stomatal lineage files; neither of these constructs produced ectopic stomata and only rarely induced extra divisions (Fig. S1).

Comparative analysis of protein domains between the orthologs reveals that BdSPCH1 and BdSPCH2 share the bHLH and a C-terminal SMF domain with AtSPCH but have a shorter MAPK target domain (MPKTD) and, strikingly, have no protein degradation-associated PEST domain (Fig. 4*A* and Fig. S9) (18). These structural differences may explain why BdSPCH1/2 but not

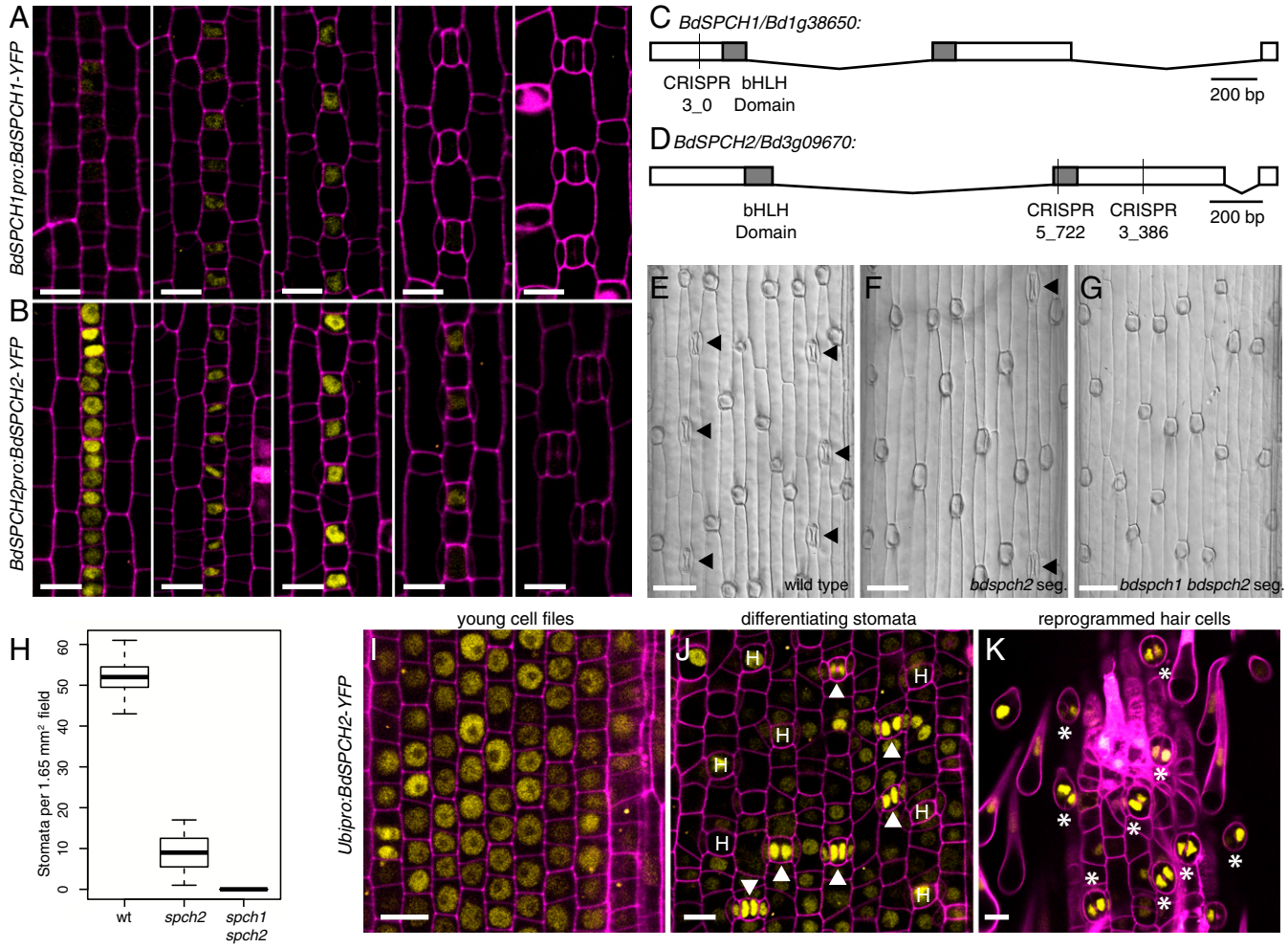

Fig. 3. *BdSPCH1* and *BdSPCH2* are partially redundant and determine stomatal fate. (*A*) *BdSPCH1pro:BdSPCH1-YFP* expression during stomatal development, peaking in late GMCs. (*B*) *BdSPCH2pro:BdSPCH2-YFP* expression during stomatal development is stronger and earlier than *BdSPCH1* expression. All confocal images show the third leaf of a T1 plant at 12 dpg. (*C* and *D*) Gene models of *BdSPCH1* (*C*) and *BdSPCH2* (*D*) showing sites of CRISPR targeting (vertical lines) and bHLH domains (gray). (*E*) Epidermis of a phenotypically WT F2 segregant. (*F*) Epidermis of a phenotypically *bdspch2*-like F2 segregant. (*G*) Epidermis of a *bdspch1 bdspch2* double-mutant segregant. All DIC images show the first leaf of plants at 7 dpg. (*H*) Quantification of stomatal density per field of view in phenotypically WT (including *bdspch1* genotypes), *bdspch2*-like, and stomataless (*bdspch1 bdspch2*) plants using the abaxial first leaf of plants at 7 dpg. $n \geq 3$ individuals. (*I–K*) *Ubipro*-driven overexpression of *BdSPCH2-YFP*, detected in every cell, induces additional divisions in the young epidermis (*I*), produces ectopic stomata (*J*), and induces division and pore formation in hair cells (*K*) in the mature epidermis. Confocal images show the third or fourth leaf of T0 plants at 11–16 dpg. Black arrowheads in *E* and *F* indicate mature stomata; white arrowheads in *J* indicate young stomata, and "H" indicates hair cells flanked by SCs; asterisks in *K* indicate divided hair cells. For all confocal images cell walls were stained with PI. (Scale bars: 10 μm in confocal images; 50 μm in DIC images.)

AtSPCH accumulate and produce ectopic stomatal lineage phenotypes when overexpressed. BdICE1, but not AtICE1, possesses two high-fidelity MAPK target sites, P-X-S/T-P (Fig. 4*B* and Fig. S10), within its PEST domain, suggesting a potential mechanism for its lineage-restricted protein accumulation when overexpressed.

BdSCRM2 is quite different from both AtICE1 and AtSCRM2; its N-terminal extension is short, and it possesses neither KRAAM nor PEST domains (Fig. 4*C* and Fig. S11), but it can substitute for *BdICE1* in producing stomata (Fig. S3). In *Arabidopsis*, the KRAAM domain was considered critical for function because AtICE1 and AtSCRM2 are made hyperactive by the substitution of a single residue (R > H); these "scrm-D" alleles produce an epidermis consisting solely of stomata (5). However, recreating this substitution in the equivalent of the KRALL domain in *BdICE1* (*Ubipro:YFP-BdICE1*^{scrmD}) failed to drive a massive conversion of epidermal cells into stomata, resulting only in occasional stomatal pairs and triplets (Fig. S12). Taken together, these findings suggest that the importance of this protein domain and its surmised role in stabilizing heterodimer interaction may be specific to Brassicaceae.

Discussion

Grasses display unique stomatal morphologies, patterns, and lineage behaviors, but our genetic screens revealed conserved transcriptional factors as key regulators of their stomatal fates. This unexpected similarity in gene content allowed us to refine our understanding of the function of stomatal bHLH transcription factors and suggest alternatives to what might be predicted from analysis in *Arabidopsis* alone. We see two cases in which paralogs are used in the same general process but have different specific functions. Although *AtICE1* and *AtSCRM2* are largely redundant and act throughout stomatal development, *BdICE1* and *BdSCRM2* act as true paralogs—potentially because of the more ancient duplication—with distinct functional requirements during stomatal development: *BdICE1* is required to establish stomatal fate, and *BdSCRM2* is required for differentiation of stomatal complexes.

Because the group Ia bHLH family is described in many species, there has been much speculation about the functions of the different members; most studies agree that FAMA and its fate-promoting activity were ancestral, but whether SPCH was a later add-on that

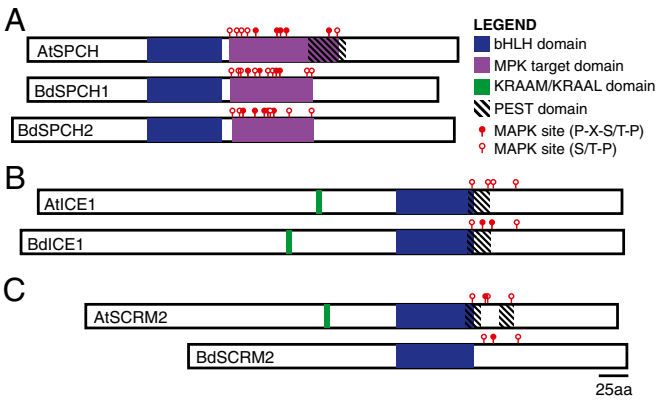

Fig. 4. Schematics of bHLH proteins, highlighting conserved and divergent domains and regulatory sites among AtSPCH, BdSPCH1, and BdSPCH2 (*A*), between AtICE1 and BdICE1 (*B*), and between AtSCRM2 and BdSCRM2 (*C*).

permits "stem cell-like" division behavior (19, 20) or whether it specifies stomatal identity (8) is controversial. Here, using the ∼140 My of divergence between grasses and dicot angiosperms, we can refine the role for SPCH; whereas the foremost function of *AtSPCH* is in driving asymmetric divisions in *Arabidopsis* (3, 20), the *BdSPCHs* have the capacity to act as fate determinants, because overexpression lines of *BdSPCH2* induce ectopic stomatal fate (Fig. 5). This altered protein behavior might result from the different origin of the stomatal lineage in the two species. The first events that distinguish the stomatal lineage from other epidermal cells in *Arabidopsis* involve the creation of dispersed meristemoids; these "point sources" of stomatal potential have unique stem cell-like and oriented asymmetric divisions maintained by *AtSPCH* (3). In contrast, in *Brachypodium*, entire files of cells obtain stomatal potential once, very early in leaf development. We can only speculate on the mechanisms leading to the change in SPCH functionality, but it is interesting that disruption of residues in *AtSPCH's* MPKTD allows SPCH to acquire the fate-determining behavior normally associated with *AtMUTE* (4, 20).

Physically asymmetric divisions are characteristic of epidermal lineages in *Brachypodium*, both in root (21) and shoot. The default cell fate of the smaller cell in the root and shoot epidermis is the hair cell (Fig. 5*A*) (21), but the expression of *BdICE1* in combination with *BdSPCH2* and *BdSPCH1* acts as a true fate "switch" (22) in the shoot to superimpose stomatal fate and increased cell divisions in specific cell files (Fig. 5*A*). Support for this hypothesis is that *bdspch1 bdspch2* leaves have WT numbers of cell files (WT = 127 ± 3.4; *bdspch2* = 128.3 ± 6; *bdspch1 bdspch2* = 131 ± 1), but these files produce hair cells instead of stomata. Ectopically expressed *BdSPCH2* can convert hair cells and hair cell precursors into stomata by inducing cell division and pore formation (Figs. 3*K* and 5*A* and Movie S2). We do not know what determines where the stomatal fate module is expressed, but the positioning might be guided by signaling originating from leaf veins, because stomatal rows always flank veins. Positional signals originating outside the stomatal lineage also might explain why *BdSPCH1/2* and *BdICE1* genes are expressed independently of each other. It is interesting that we see

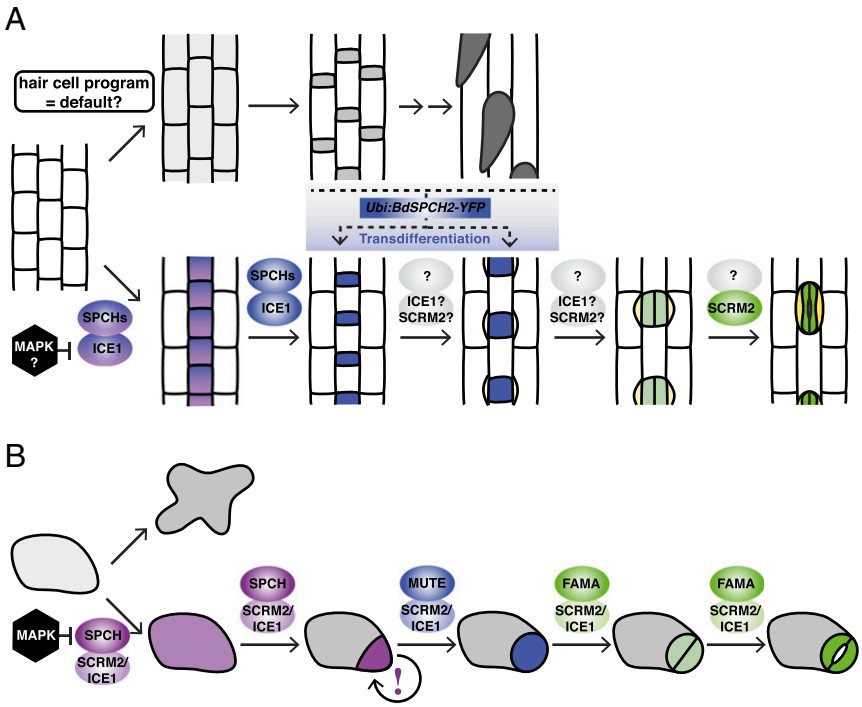

Fig. 5. Model for the gene regulatory network in grass and dicot stomatal initiation. (*A*) Model of stomatal development in *Brachypodium*. An epidermal program induces asymmetric division in all cell files, and the smaller daughter cell, by default, becomes a hair cell. Expression of the stomatal module (BdSPCHs and BdICE1) in a specific cell file acts as a switch to establish stomatal fate. The stomatal files proliferate more than hair cell files and produce smaller cells. However, the proliferation phase (purple) is much shorter than in *Arabidopsis* and is restricted to the base of the leaf. *BdSPCH2* has the potential to trans-differentiate hair precursors and even mature hair cells to stomata and therefore acts as a true GMC fate determinant (blue phase). Finally, *BdSCRM2* promotes differentiation of the grass stomatal complex (green phase). Transcription factors are color coded to match the stage at which they act; intermediate steps could also be (partly) regulated by *BdSPCH1/2* and *BdICE1* (gray ovals), but early-arrest phenotypes preclude definitive assignment here. (*B*) Model of stomatal development in *Arabidopsis* for comparison, with color-coded developmental stages and factors. *AtSPCH* establishes the stomatal lineage and controls asymmetric, stem cell-like divisions of meristemoids (purple phase). *AtMUTE* regulates the exit of stem-cell behavior and defines stomatal fate by establishing the GMC (blue phase). Finally, *AtFAMA* controls the single symmetric GMC division and GC differentiation (green phase). AtICE1 and AtSCRM2 are redundant heterodimerization partners of AtSPCH, AtMUTE, and AtFAMA and are expressed and required throughout stomatal development in *Arabidopsis*.

examples of plants subjecting only one heterodimerization partner to tight posttranslational control; whether a specific functionality is made possible by targeting the SPCH or ICE1 clade in different species or whether targeting either one is sufficient for control of stomatal patterning is not yet known, but it is intriguing to speculate that the acquisition or loss of phosphorylation target sites and degradation domains might dynamically shape the regulation of the stomatal module throughout the plant kingdom.

We have shown that although the same gene families are involved in establishing the stomatal lineage in *Arabidopsis* and grasses, the structure, function, and regulation of the proteins encoded by these genes parallel differences in lineage origin and form between the different plant families. From an evolutionary point of view, much of the research in the evolution of gene regulatory networks has focused on *cis*-regulatory element changes (22, 23). Although these changes undoubtedly are an important feature of the networks, our investigations revealed changes in protein function and regulation that shape the stomatal development initiation network. It is possible that our choice of the stomatal lineage as a subject emphasizes this mode of regulation. Other comparative studies have focused on fundamental body-plan regulators such as HOX genes, which may be tightly constrained (22, 23), or end-point regulators such as pigment patterns in insect wings in which the genes regulate relatively small and defined downstream outputs (24). The stomatal module sits at an intermediate place between these two; the stomatal lineage is a postembryonic creation and is highly adaptable to environmental conditions, but the bHLHs still regulate hundreds to thousands of targets (25, 26).

The grasses are an extraordinarily successful and economically important plant group (27), and some have speculated that their evolutionary success results, in part, from developmental innovations that increase stomatal responsiveness (1). The core stomatal bHLH transcription factors identified in *Arabidopsis* are found in all major crop plants (8), and mutations in rice homologs of *SPCH* and *FAMA* were reported to affect stomatal production (14). Here, focusing on the stomatal initiation genes individually and as an integrated unit, we see how they may be alternatively wired to generate different stomatal patterns and densities. Because stomata are at the plant–atmosphere interface and regulate photosynthetic and water use efficiency, the stomatal development "kernel" becomes an attractive target for genetic strategies to improve plant productivity and drought resistance to satisfy a growing need for food and energy in a changing climate.

Methods

Plant Material. *Brachypodium* line Bd21-3 was used for all experiments (28). The *stl* mutant was recovered from the M3 generation of an EMS mutagenized population (jgi.doe.gov/our-science/science-programs/plant-genomics/brachypodium/). For details on the mutant screen, growth conditions, crosses, molecular procedures, and data analysis, see *SI Methods*.

Cloning, Plant Transformation, and Microscopy. CRISPR constructs were designed using the vector system and following the design protocol in ref. 15. All reporter and overexpression constructs were generated using the pIPKb vector series (29). *Brachypodium* calli were transformed with AGL1 *Agrobacterium*, selected based on hygromycin resistance, and regenerated according to standard protocols (30). For confocal imaging, the division zone of emerging second (6 or 7 dpg) or third (11 or 12 dpg) leaves was counterstained with propidium iodide (PI) and imaged on a Leica SP5 confocal microscope. For differential interference contrast (DIC) imaging, leaf tissue (generally the distal 1.5–2 cm of the first or second leaf blade of 6–8 dpg or 11–12 dpg plants, respectively) was fixed, cleared, and examined using a Leica DM2500 microscope. For details on molecular cloning and plant transformation, please refer to *SI Methods*. All primers are listed in Table S1.

ACKNOWLEDGMENTS. We thank C. Ballenger and M. X. Anleu Gil for technical support, J. L. Matos for help establishing *Brachypodium* in our laboratory, and H. Lindner for comments on the manuscript. This work is supported by Swiss National Science Foundation Fellowship P2ZHP3_151598 (to M.T.R.) and Life Science Research Foundation Grant GBMF2550.05 (to M.T.R.). E.A. was a National Science Foundation graduate research fellow, and D.C.B. is an Investigator of the Howard Hughes Medical Institute. The work conducted by the US Department of Energy Joint Genome Institute is supported by the Office of Science of the US Department of Energy under Contract DE-AC02-05CH11231.

1. Franks PJ, Farquhar GD (2007) The mechanical diversity of stomata and its significance in gas-exchange control. *Plant Physiol* 143(1):78–87.
2. Ohashi-Ito K, Bergmann DC (2006) *Arabidopsis* FAMA controls the final proliferation/differentiation switch during stomatal development. *Plant Cell* 18(10):2493–2505.
3. MacAlister CA, Ohashi-Ito K, Bergmann DC (2007) Transcription factor control of asymmetric cell divisions that establish the stomatal lineage. *Nature* 445(7127):537–540.
4. Pillitteri LJ, Sloan DB, Bogenschutz NL, Torii KU (2007) Termination of asymmetric cell division and differentiation of stomata. *Nature* 445(7127):501–505.
5. Kanaoka MM, et al. (2008) SCREAM/ICE1 and SCREAM2 specify three cell-state transitional steps leading to *Arabidopsis* stomatal differentiation. *Plant Cell* 20(7):1775–1785.
6. Torii KU (2015) Stomatal differentiation: The beginning and the end. *Curr Opin Plant Biol* 28:16–22.
7. Lampard GR, Macalister CA, Bergmann DC (2008) *Arabidopsis* stomatal initiation is controlled by MAPK-mediated regulation of the bHLH SPEECHLESS. *Science* 322(5904):1113–1116.
8. Ran JH, Shen TT, Liu WJ, Wang XQ (2013) Evolution of the bHLH genes involved in stomatal development: Implications for the expansion of developmental complexity of stomata in land plants. *PLoS One* 8(11):e78997.
9. Olsen JL, et al. (2016) The genome of the seagrass *Zostera marina* reveals angiosperm adaptation to the sea. *Nature* 530(7590):331–335.
10. Sage RF, Sage TL, Kocacinar F (2012) Photorespiration and the evolution of C4 photosynthesis. *Annu Rev Plant Biol* 63(1):19–47.
11. Cartwright HN, Humphries JA, Smith LG (2009) PAN1: A receptor-like protein that promotes polarization of an asymmetric cell division in maize. *Science* 323(5914):649–651.
12. Zhang X, et al. (2012) Identification of PAN2 by quantitative proteomics as a leucine-rich repeat-receptor-like kinase acting upstream of PAN1 to polarize cell division in maize. *Plant Cell* 24(11):4577–4589.
13. Facette MR, et al. (2015) The SCAR/WAVE complex polarizes PAN receptors and promotes division asymmetry in maize. *Nat Plants* 1(2):14024.
14. Liu T, Ohashi-Ito K, Bergmann DC (2009) Orthologs of *Arabidopsis thaliana* stomatal bHLH genes and regulation of stomatal development in grasses. *Development* 136(13):2265–2276.
15. Miao J, et al. (2013) Targeted mutagenesis in rice using CRISPR-Cas system. *Cell Res* 23(10):1233–1236.
16. Horst RJ, et al. (2015) Molecular framework of a regulatory circuit initiating two-dimensional spatial patterning of stomatal lineage. *PLoS Genet* 11(7):e1005374.
17. Chinnusamy V, et al. (2003) ICE1: A regulator of cold-induced transcriptome and freezing tolerance in *Arabidopsis*. *Genes Dev* 17(8):1043–1054.
18. Rogers S, Wells R, Rechsteiner M (1986) Amino acid sequences common to rapidly degraded proteins: The PEST hypothesis. *Science* 234(4774):364–368.
19. MacAlister CA, Bergmann DC (2011) Sequence and function of basic helix-loop-helix proteins required for stomatal development in *Arabidopsis* are deeply conserved in land plants. *Evol Dev* 13(2):182–192.
20. Davies KA, Bergmann DC (2014) Functional specialization of stomatal bHLHs through modification of DNA-binding and phosphoregulation potential. *Proc Natl Acad Sci USA* 111(43):15585–15590.
21. Kim CM, Dolan L (2011) Root hair development involves asymmetric cell division in *Brachypodium distachyon* and symmetric division in *Oryza sativa*. *New Phytol* 192(3):601–610.
22. Davidson EH, Erwin DH (2006) Gene regulatory networks and the evolution of animal body plans. *Science* 311(5762):796–800.
23. Carroll SB (2008) Evo-devo and an expanding evolutionary synthesis: A genetic theory of morphological evolution. *Cell* 134(1):25–36.
24. Parchem RJ, Perry MW, Patel NH (2007) Patterns on the insect wing. *Curr Opin Genet Dev* 17(4):300–308.
25. Lau OS, et al. (2014) Direct roles of SPEECHLESS in the specification of stomatal self-renewing cells. *Science* 345(6204):1605–1609.
26. Pillitteri LJ, Peterson KM, Horst RJ, Torii KU (2011) Molecular profiling of stomatal meristemoids reveals new component of asymmetric cell division and commonalities among stem cell populations in *Arabidopsis*. *Plant Cell* 23(9):3260–3275.
27. Kellogg EA (2001) Evolutionary history of the grasses. *Plant Physiol* 125(3):1198–1205.
28. Vogel J, Hill T (2008) High-efficiency *Agrobacterium*-mediated transformation of *Brachypodium distachyon* inbred line Bd21-3. *Plant Cell Rep* 27(3):471–478.
29. Himmelbach A, et al. (2007) A set of modular binary vectors for transformation of cereals. *Plant Physiol* 145(4):1192–1200.
30. Bragg JN, et al. (2012) Generation and characterization of the Western Regional Research Center Brachypodium T-DNA insertional mutant collection. *PLoS One* 7(9):e41916.
31. Hong SY, Seo PJ, Yang MS, Xiang F, Park CM (2008) Exploring valid reference genes for gene expression studies in *Brachypodium distachyon* by real-time PCR. *BMC Plant Biol* 8(1):112.
32. Ream TS, et al. (2014) Interaction of photoperiod and vernalization determines flowering time of *Brachypodium distachyon*. *Plant Physiol* 164(2):694–709.
33. Curtis MD, Grossniklaus U (2003) A gateway cloning vector set for high-throughput functional analysis of genes in planta. *Plant Physiol* 133(2):462–469.